CRYSTALLINITY PREDICTION OF SHORT CARBON FIBRE REINFORCED POLYAMIDE 6 COMPOSITES MANUFACTURED BY FUSED FILAMENT FABRICATION

Zhu, Yifan; Van Daele, Lenny; Van Vlierberghe, Sandra; Pyl, Lincy

Published in:
CRYSTALLINITY PREDICTION OF SHORT CARBON FIBRE REINFORCED POLYAMIDE 6 COMPOSITES MANUFACTURED BY FUSED FILAMENT FABRICATION

DOI:
https://doi.org/10.5075/epfl-298799_978-2-9701614-0-0

Publication date:
2022

Document Version:
Accepted author manuscript

Composites Meet Sustainability – Proceedings of the 20th European Conference on Composite Materials, ECCM20. 26-30 June, 2022, Lausanne, Switzerland

CRYSTALLINITY PREDICTION OF SHORT CARBON FIBRE REINFORCED POLYAMIDE 6 COMPOSITES MANUFACTURED BY FUSED FILAMENT FABRICATION

Yifan, Zhu[a,b], Lenny, Van Daele[c], Sandra, Van Vlierberghe[c], Lincy, Pyl[a]
a: Department of Mechanics of Materials and Constructions (MeMC), Vrije Universiteit Brussel (VUB), Pleinlaan 2, B-1050
Brussels, Belgium – yifan.zhu@vub.be
b: SIM vzw, Technologiepark 48, B-9052 Zwijnaarde, Belgium
c: Polymer Chemistry and Biomaterials Group (PBM), Centre of Macromolecular Chemistry (CMaC), Department of Organic and Macromolecular Chemistry, Ghent University, Krijgslaan 281 S4-bis, B-9000 Ghent, Belgium

Abstract: *Polymer additive manufacturing has transformed itself from a technology that is mainly focused on rapid prototyping to a widely received manufacturing technique for highly customised products. In fused filament fabrication (FFF), due to the fast heating and cooling of the polymer, the printed part's crystallinity and mechanical properties are inevitably affected. This research proposes a numerical approach to predict the final crystallinity for FFF printed polyamide 6/short carbon fibre composite. To do so, samples were built with the FFF technique with their temperature history recorded by infrared camera measurements. Differential scanning calorimetry (DSC) was conducted on the FFF filament to calibrate the numerical model. Temperature history was used as input for the model and the printed part's final crystallinity is predicted. Tensile tests were carried out to examine the influence of crystallinity on the printed part's mechanical performance.*

Keywords: Fused filament fabrication; Short fibre reinforced thermoplastic; Crystallinity

1. Introduction

The availability and accessibility of fused filament fabrication (FFF) have made it a popular choice among the public and some industries. Despite the ease of having access to such technology, the intrinsic complexity of this manufacturing process remains an obstacle to fully unleash its potential. A direct correlation between the inputs and the performance of the final product is still not fully understood. It is known that higher crystallinity leads to an increased modulus of the material [1]. Being able to predict the level of crystallinity in the printed part is an interesting development, as it economises the cost of testing and gives a non-destructive way of estimating the level of crystallinity.

In literature, several approaches were proposed to predict the crystallinity evolution of FFF printed semi-crystalline polymers. Pu et al. [2] considered the crystallisation process to be quiescent and used the Schneider rate equations. The predicted level of crystallinity was correlated to the mechanical performance of the printed part. Samy et al. [3] utilised the Nakamura crystallisation kinetics model to investigate the evolution of crystallinity. The printed part's distortion and residual stress were deduced from the calculated crystallinity.

In this study, the crystallinity development of short carbon fibre reinforced polyamide 6 processed by FFF is examined. The prediction is done by employing Velisaris' crystallisation model [4]. The predicted level is compared against the experimental one and similar values

were found. The influence of different levels of crystallinity on mechanical performance was examined by tensile tests.

2. Experimental

2.1 Material and manufacturing

The material used for this study was Onyx from Markforged, a type of filament made of polyamide 6 with short carbon fibre reinforcement. The diameter of the filament is 1.75mm and it is constantly stored in a desiccator or dry box to prevent moisture absorption. The detailed info like molecular weight or chemical composition of Onyx is not disclosed by Markforged.

Markforged Mark Two printer was used for the manufacturing of the samples. The sample dimension is 70 x 10 x 0.7 mm^3 (L x H x T) and the printing path for each layer could be seen in figure 1a, the sample is made to have two parallel tracks per layer. The layer thickness for the printing was set to be 200 µm and in total each sample has 50 layers. Other key process parameters like printing speed, nozzle temperature or extrusion speed are not adjustable by users and Markforged's default slicer software Eiger sets them automatically.

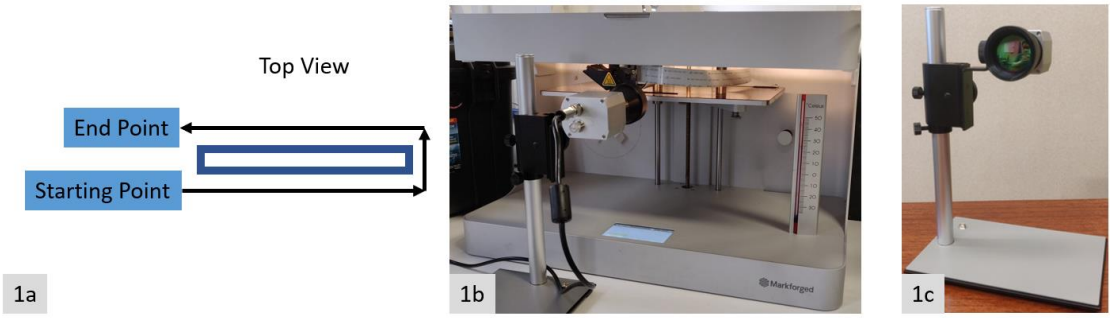

Figure 1a. Layer printing path of the sample, 1b. The setup used during printing, 1c. Infrared camera.

3D printing of samples was performed under two environmental conditions. The first one is printing without the cover which exposes the entire build chamber to the ambient air. In the second condition, the build chamber is covered with a plastic envelope that traps the extruder's heated air. A thermometer is placed near the build plate to measure the chamber temperature. In the first and second condition, the chamber temperature was 25°C and 35°C, respectively.

2.2 Process temperature monitoring

The temperature measuring during the printing process was performed with an Optris PI640i infrared camera equipped with microscope optics. The camera detects infrared signals at a spectral range of 8 – 14 µm and records at a resolution of 640 x 480 pixels, the maximum framerate at this resolution is 32 Hz. At a working distance of 100 mm, it has a field of view (FOV) of 25.4 x 17.5 mm^2 which provides a spatial resolution of 25.2 µm per pixel. Given the layer thickness is 200 µm, 7 measurements could be made per height of a layer. The camera was set up to point at the front face of the sample. Figure 1b shows the setup during printing while figure 1c is the infrared camera used. The lengthwise middle section of the sample was inside the FOV and it corresponds to the gauge section for tensile testing. An emissivity value of 0.95 is adopted in this study [5]. Temperature measurements in the concave regions in

between layers give underestimated values as the view angle between the normal surface and the camera gets close to 90°. To circumvent this, measurement of layer temperature was done at the mid-height pixel of the layer. The recorded temperature data was used as input for the crystallinity calculation.

2.3 Differential scanning calorimetry

To obtain the coefficients for calibrating the numerical model and predict the final crystallinity, isothermal and non-isothermal crystallisation experiments are conducted with standard differential scanning calorimetry (DSC) on the Onyx filament. For the isothermal tests, crystallisation temperatures of 165°C, 170°C, 175°C and 180°C were chosen. The samples quickly cool from 275°C to the desired isothermal temperature at a rate of 50°C/min. It then holds at the isothermal temperature for an extra 60 minutes. The non-isothermal tests were carried out at cooling rates of 5°C, 10°C, 20°C, 30°C, 40°C, and 50°C per minute. All samples cool from 275°C at the specific cooling rate to 40°C and the experiment is concluded.

To find the final crystallinity of the printed samples and compare the experimental results with the prediction, modulated differential scanning calorimetry (mDSC) analyses were used. Tests were made up of a single heating run at a heating rate of 2°C/min to 275°C with modulation of ±0.32°C every 60 seconds. The level of absolute crystallinity (X_{abs}) of the printed samples was then calculated from equation 1.

$$X_{abs} = \frac{\Delta H_f - \Delta H_{cc}}{\Delta H_f^{\infty}} \quad (1)$$

Where ΔH_f represents the enthalpy of fusion, ΔH_{cc} is the cold crystallisation enthalpy and ΔH_f^{∞} is the enthalpy of fusion for fully crystalline polyamide 6. Due to the material being a blend of around 90% by weight polyamide 6 and 10% short carbon fibre [6], the mixture rule was used and obtained a value of 169.2 J/g.

The equipment selected to conduct both the mDSC and DSC experiments was Q2000 from TA instruments installed with refrigerated cooling systems. All experiments were performed under a nitrogen environment. To process the experimental data, Universal Analysis from TA Instruments was used.

2.4 Tensile test setup

Tensile tests were performed on printed samples to examine the influence of the level of crystallinity on mechanical properties. An Instron 5885 testing system equipped with mechanical grips and a 10 kN load cell was used for the tensile tests. All tests were performed under displacement control at a crosshead displacement rate of 1 mm/min to avoid any dynamical effect. A 2620-601 dynamic extensometer from Instron was utilized for the strain measurement. For each environmental condition (build chamber without cover and with cover), 4 tensile samples were tested.

3. Modelling

Velisaris' phenomenological model captures both the primary and secondary stages of polymers crystallisation [7]. For the detailed derivation of the model, readers are referred to the original paper. The applicability of this model to additively manufactured composites was demonstrated by Brenken et al. [8] on 50% by weight carbon fibre reinforced polyphenylene

sulphide. Tierney et al. [9] validated the appropriateness of this model by predicting the final crystallinity of polyether ether ketone (PEEK)/carbon fibre composite.

The model is shown from equation 2 till 4:

$$w_1 + w_2 = 1 \tag{2}$$

$$X_{vc} = X_{vc\infty}(w_1 F_{vc1} + w_2 F_{vc2}) \tag{3}$$

$$F_{vci} = 1 - exp\left\{-C_{1i}\int_0^t T * exp\left[\frac{-C_{2i}}{T - T_g + T_{ci}} - \frac{C_{3i}}{(T(T_{mi} - T)^2)}\right] n_i \tau^{n_i - 1} d\tau\right\} \tag{4}$$

$$i = 1{,}2$$

Where $X_{vc\infty}$ is the maximum level of crystallinity achievable by the material and X_{vc} represents the actual level of crystallinity. The primary and secondary crystallisation mechanisms are described by function F_{vc1} and F_{vc2}, and the extent of each mechanism relative to the other is given by the weight factor w_1 and w_2. Inside functions $F_{vci,}$ parameter C_{1i} describes the crystallisation rate's temperature dependence, C_{2i} is associated with the temperature dependence of the growth mechanism and C_{3i} is related to the enthalpy of nucleation. n_i is the Avrami exponent for each mechanism and is extracted from the isothermal crystallisation experiments. T, T_g are used to represent the temperature of the process and glass transition temperature of the material, respectively. T_{mi}, T_{ci} are the melting temperature and empirical fitting temperature for primary or secondary crystallisation, respectively. From the mDSC heating run, the glass transition temperature of the material was identified at 44°C.

4. Results and discussion

4.1 Infrared thermal imaging

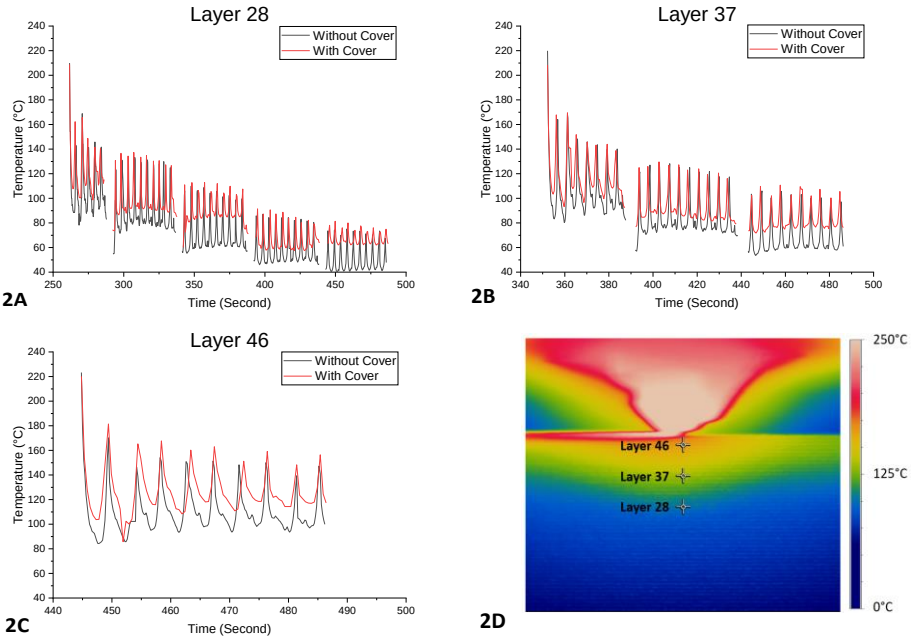

Figure 2. 2a – 2c, Temperature profile of the points from just extruded till the end of printing. 2d, Locations of the measuring points.

Three measuring points, situated at the midpoint in terms of both length and height of each layer, were chosen on layer 28, 37 and 46, as shown in figure 2D. The temperature history of these three points could be observed in figure 2A to 2C respectively.

The fresh extrudate has a temperature above 200°C and it drops to around 100°C within one second. As the nozzle travels to print the backside of the layer, the next peak appears when the new extrudate is in contact with the front track at the measuring point. Thus, every two consecutive peaks represent a layer that is finished. Due to the mechanism of the Markforged printer, the machine lowers the build plate by 4 mm for around 5 seconds when every 5 layers are printed. This causes a portion of the sample to disappear from the FOV of the infrared camera and creates discontinuities in the measured temperature profile as can be seen in figure 2a and 2b. After the 5 seconds of disappearance, the build plate returns to the previous height. It is observed that the layer temperature decreases as it is away from the nozzle. As more layers are deposited, the measured points get further away from the top layer and hence an overall cooling trend is observed. By comparing the temperature profile of printing with or without cover, it could be seen that both conditions have similar peak temperatures. However, printing with cover has a slower cooling rate as demonstrated in the higher valley temperatures in between successive peaks, this is due to the higher build chamber temperature which creates a lower temperature gradient.

4.2 Crystallisation analysis

The absolute and relative crystallisation evolution for filaments that underwent non-isothermal crystallisation at different cooling rates is shown in figure 3. All plots have a typical sigmoidal shape and with a higher cooling rate, the plot translates towards the left which means that the onset and end of crystallisation are at lower temperatures. The maximum crystallinity achieved is 23.57% for filaments cooled at 5°C/min and this value is used in the model's calibration.

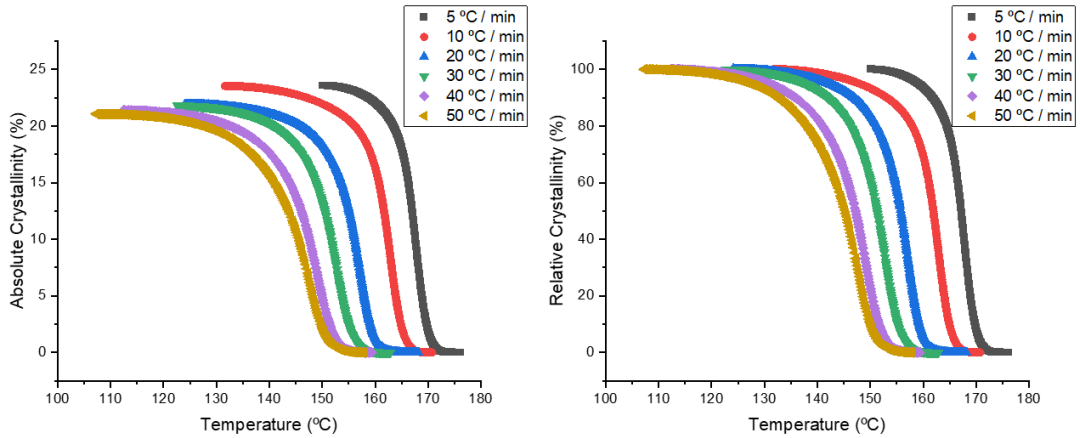

Figure 3. Absolute and relative crystallinity evolution for Onyx filament at various cooling rates.

Equations 5 and 6 are used to compute the absolute crystallinity and relative crystallinity , respectively.

$$X_{abs} = \frac{\Delta H_C}{\Delta H_f^{\infty}} \quad (5)$$

$$X_{rel}(t) = \frac{\int_{t_o}^{t} (\frac{dH}{dt})\, dt}{\int_{t_e}^{t} (\frac{dH}{dt})\, dt} \quad (6)$$

Where ΔH_C represents the enthalpy of crystallisation and ΔH_f^{∞} is the enthalpy of fusion for fully crystalline polyamide 6/short carbon fibre composite. Concerning equation 6, t_o and t_e are the onset crystallisation and end crystallisation time, *H* is the heat flow, and *t* represents the time during crystallisation. DSC results from the isothermal crystallisation experiments are processed and used to create Avrami plots [10] as shown in figure 4. The Avrami exponents are derived from the slope of the plots.

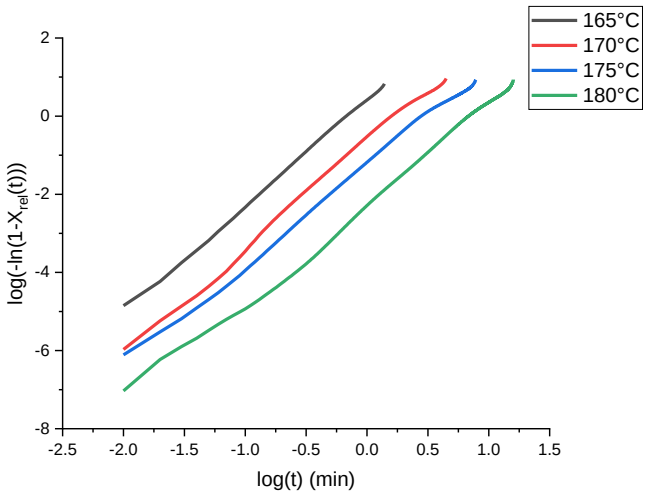

Figure 4. Avrami plot for isothermal crystallisation at various temperatures.

4.3 Modelling result

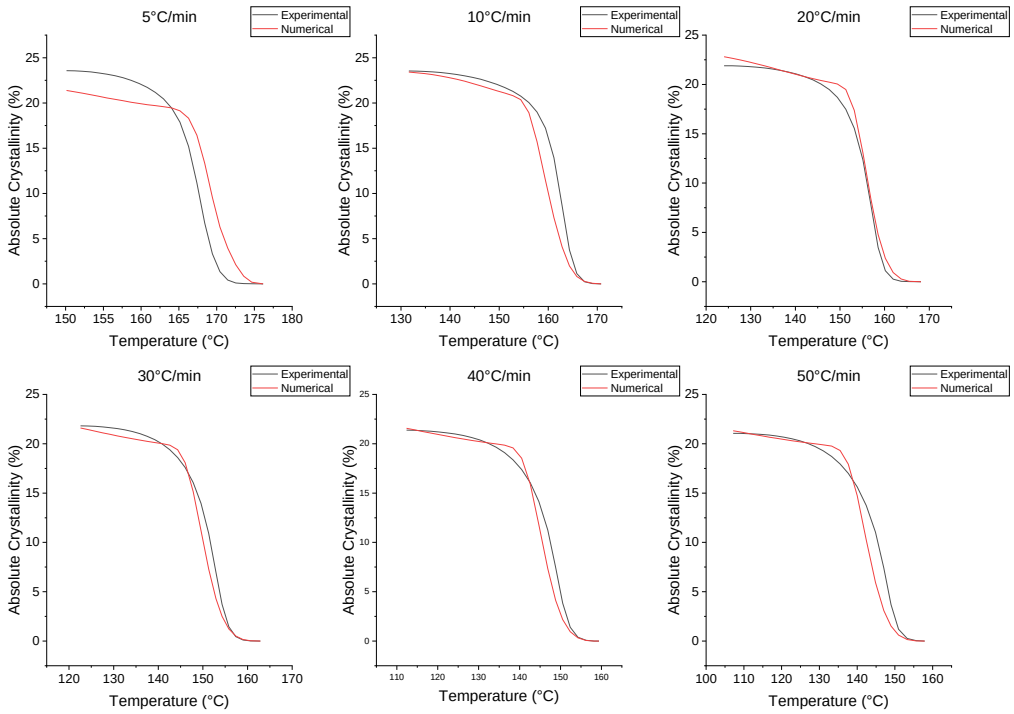

Figure 5. The numerical model fitted to non-isothermal crystallisation data.

Data obtained from both the isothermal and non-isothermal crystallisation experiments are used to characterize all the parameters for the numerical model. From the isothermal result, the calculated Avrami exponents for each mechanism are adopted. The model was then fitted to the non-isothermal experimental result at all cooling rates by using Matlab. Figure 5 shows the experimental and fitted curve of the absolute crystallinity as a function of temperature. From the curve fitting, all the parameters in equation 4 to 6 are found. The time-temperature data from the infrared recording are then used as input for the crystallinity prediction of the printed samples. Table 2 shows the results of the prediction compared to the experimental results.

Table 2: Prediction of absolute crystallinity of printed samples.

Condition	$X_{experiment,abs}$ [%]	$X_{prediction,abs}$ [%]	Deviation [%]
Printed With Cover	19.44	21.99	+ 13.12
Printed Without Cover	18.64	19.39	+ 4.02

The predicted values have deviation up to 13.12% from the experimental result which demonstrated the approach's feasibility in estimating crystallinity. For both conditions, the prediction of absolute crystallinity of printed samples is higher than the experimentally determined crystallinity. This could be due to the model being fitted to filament data at cooling rates up to 50°C/min. The temperature gradient during fused filament fabrication is more than 10^2 higher (> 5000°C/min). Such difference may cause the model to overestimate the level of crystallinity. According to Winkelmann et al. [11], further improvement to the model can be done by fitting to experimental data at the anticipated cooling rate by using flash DSC.

4.4 Mechanical properties

Table 3 summarizes the tensile properties of the printed samples. Samples printed in a build chamber with cover condition have marginally higher values in all tensile properties. This is attributed to the slightly higher level of crystallinity which gives it more mechanical strength. However, lower ultimate strain is observed on samples with lower crystallinity which is not coherent with the literature finding [1]. This peculiarity is hypothesised to be due to the surface effect as samples printed without cover tend to have a rougher surface.

Table 3: Tensile strength of printed samples.

Condition	Young's modulus [GPa]	Ultimate stress [MPa]	Ultimate strain [%]
Printed With Cover	1.45 ± 0.12	48.04 ± 0.17	24.03 ± 1.13
Printed Without Cover	1.39 ± 0.19	46.40 ± 0.13	22.48 ± 1.97

5. Conclusion

This study presented a methodology for estimating the level of crystallinity of polyamide 6/short carbon fibre composite made by FFF. The infrared thermal data show that printing with a cover creates a relatively slower cooling rate as compared to printing without. Also, a feasible way of estimating the final crystallinity of the printed part by using thermal history along with the calibrated numerical model is demonstrated. Fitting non-isothermal

crystallisation data at a much higher cooling rate could further enhance such a model and improve its accuracy.

Acknowledgements

The authors acknowledge the support of the Agency for Innovation and Entrepreneurship Flanders via the Strategic Initiative Materials in Flanders in the framework of the SIM-SBO PET2VALUE project, running in the NANOFORCE program.

6. Reference

1. Babs V, Amalia K, Lincy P, Sandra V.(2022). Effect of extrusion and fused filament fabrication processing parameters of recycled poly(ethylene terephthalate) on the crystallinity and mechanical properties. Additive Manufacturing 2022; 50: 102518

2. Pu, J, McIlroy C, Jones A, Ashcroft I. Understanding mechanical properties in fused filament fabrication of polyether ether ketone. Additive Manufacturing 2021; 37:101673.

3. Samy A, Golbang A, Harkin E, Archer E, McIlhagger A. Prediction of part distortion in Fused Deposition Modelling (FDM) of semi-crystalline polymers via COMSOL: Effect of printing conditions. CIRP Journal Of Manufacturing Science And Technology 2021; 33: 443-453.

4. Velisaris N, Seferis C. Crystallization kinetics of polyetheretherketone (peek) matrices. Polym Eng Sci 1986; 26: 1574-1581

5. Faust L, Kelly G, Jones D, Roy D. Effects of Coefficient of Thermal Expansion and Moisture Absorption on the Dimensional Accuracy of Carbon-Reinforced 3D Printed Parts. Polymers 2021; 13: 3637.

6. Pascual C, Iragi M. An approach to analyse the factors behind the micromechanical response of 3D-printed composites. Composites Part B: Engineering 2020; 186: 107820.

7. Kelly C, Jenkins M. Modeling the crystallization kinetics of polymers displaying high levels of secondary crystallization. Polymer Journal 2021; 54(3): 249-257.

8. Brenken B, Barocio E, Favaloro A, Kunc V, Pipes R. Development and validation of extrusion deposition additive manufacturing process simulations. Additive Manufacturing 2018; 25: 218-226.

9. Tierney J, Gillespie Jr J. Crystallization kinetics behavior of PEEK based composites exposed to high heating and cooling rates. Composites Part A: Applied Science And Manufacturing 2003; 35(5): 547-558.

10. Lorenzo A, Arnal M, Albuerne J, Müller A. DSC isothermal polymer crystallization kinetics measurements and the use of the Avrami equation to fit the data: Guidelines to avoid common problems. Polymer Testing 2007; 26(2): 222-231.

11. Winkelmann F, Hein R. Further development of a simulation model for the description of the crystallization kinetics of semi-crystalline thermoplastics. NAFEM World Congress. 2021.

12. Brenken B. Extrusion Deposition Additive Manufacturing of Fiber Reinforced Semi-Crystalline Polymers. Purdue University ProQuest Dissertations Publishing. 2017.

